Rigid Body Collision Model for Submunition Dispersion Simulation

James W. Purvis*
Sandia National Laboratories, Albuquerque, New Mexico

A collision model for use in digital computer simulations of submunition dispersion is presented. The model consists of three distinct parts: a collision decision hierarchy, a solid body model, and momentum exchange equations. The collision decision hierarchy is a simulation of the human observation process for detecting bodies in contact. The solid body model, used to determine contact points, is restricted to bodies of revolution. Exact analytical equations are derived for the exchange of linear and angular momentum during a collision. The equations account for coefficients of restitution other than unity. Some computed results are presented.

Nomenclature

b_{ij}	= direction cosines
C_R	= coefficient of restitution
E_R	= kinetic energy of rotation
E_T	= kinetic energy of translation
f_i	= elastic collision force vector
G	= collision impulse magnitude
G_i	= collision impulse vector, Eq. (14)
H_i	= angular momentum vector (body axes)
I_{ij}	= inertia tensor
J_{ij}	= inertia tensor inverse, Eq. (26)
L	= cylinder length
m	= mass
n_i	= unit vector
n_i^c	= projection of unit vector, Eq. (5)
P_i	= linear momentum vector
Q_c	= scalar length, Eq. (7b)
Q_i	= separation vector, Eq. (4)
Q_L	= scalar length, Eq. (7a)
q_i	= impulse moment arm vector, Eq. (24)
R_i	= inertial position or separation vector
r	= sphere or cylinder radius
r_i	= position vector
r_s	= sphere radius, Fig. 2
t	= time
u_i	= velocity vector
x_s	= sphere location relative to body c.g., Fig. 2
δ_{ij}	= unit tensor
ϵ_{ijk}	= permutation tensor
ω_i	= angular velocity vector (body axes)

Introduction

TACTICAL weapons with cluster-type warheads which contain a number of small projectiles (submunitions) are being proposed and developed with increasing frequency. Prediction of actual impact pattern distribution, particularly during preliminary design, is vital to the assessment of weapon effectiveness. The Naval Surface Weapons Center has an ongoing Cluster Warhead Technology Program, the objective of which is to develop a preliminary design methodology capable of accurate deterministic prediction of impact patterns. Such a methodology necessarily involves a six-degree-of-freedom (6DOF) multiple-body trajectory simulation program, which in turn requires accurate initial conditions for each submunition.

As noted by Brunk,[1] the initial motion of each submunition is established during the ejection and cluster breakup phase of flight, which usually involves only a few tenths of a second. Flight dynamics of individual submunitions during ejection and cluster breakup flight regimes are not easily predicted due to two major problems—aerodynamic interference and collisions. Consequently, in most trajectory simulations, the velocity and attitude of each submunition are presently determined from stochastic models or experimental data. The alternative is to model accurately, as part of the trajectory program, the ejection and cluster breakup phases, so that only the canister or parent vehicle initial conditions need to be determined.

The areodynamic interference problem has been studied extensively with respect to store separation. Several methods are available for predicting aerodynamic interference, such as Refs. 2-4, and improvements to these methods are currently under development. The remaining major modeling deficiency is the ability to predict collisions and their effects on submunition attitude. In general, the fewer the number of submunitions, the more important collision effects become with respect to dispersion patterns.

An extensive literature survey revealed a paucity of information in the area of rigid body collision models. Bayman[5] and Maryamor[6] both studied the behavior of solid bodies during collisions. The former developed a one-dimensional model of elastic behavior using Hooke's Law springs, while the latter used the compressible fluid conservation equations to investigate the effects of hypervelocity impacts. With respect to computer manipulation systems, algorithms such as that of Ref. 7 are available for determining collision free paths among polyhedral objects. The automotive and shipping industries have addressed the collision problem from the standpoints of interference-free mechanical design,[8] crashworthiness,[9] and maritime accidents.[10] Some closely related work was done by Brach,[11] who investigated the effects of impulsive moments on the postcollision paths of automobiles. The most relevant work (such as Refs. 12 and 13) has been done on the dynamics of missile stage separation, where collision and tip-off problems are encountered. However, to quote Boyse,[8] "Very little has been published which is aimed specifically at the interference checking problem."

The only general computer model for predicting collisions between aerodynamic bodies was found to be that given in Refs. 14 and 15, which appears to be the state of the art in submunition trajectory programs. Although both programs (Ref. 15 is a more advanced version of Ref. 14) include a

Presented as Paper 82-0363 at the AIAA 20th Aerospace Sciences Meeting, Orlando, Fla., Jan. 11-13, 1982; received June 9, 1981; revision received Sept. 27, 1982.

*Member of Technical Staff, Aerodynamic Department 1630.

trajectory simulation and a collision model, only the collision model is of interest in this paper.

Each body in the method of Ref. 15 is modeled in two ways—one composed of spherical, conical, cylindrical, and planar surfaces, and the other composed of a set of points. To simulate the collision process, the motion of the body points are tracked in time and checked against the surface model of other bodies. A collision occurs when one or more points penetrate any surface on another body. Impact forces are then computed which resist further penetration. The impact forces consist of a surface normal component f_n, which acts along the surface normal vector at the impact point, and a surface tangent component f_t, which acts opposite to the relative velocity component tangent to the surface. The normal force is proportional to the depth of penetration; that is, $f_n = k\delta$, where δ is the depth of penetration and k is a property of the surface.

The collision model is very general in that bodies with quite complex shapes can be described. If a large number of points are used to define the body, collision points can be determined very accurately. Unfortunately, when a large number of points are used to define a body, the input data and computational requirements increase substantially. In cases where it is necessary to reduce the amount of input data or decrease the computational requirements, a "man-in-the-loop" mode is provided. In this mode, an observer can monitor a computer graphics depiction of the simulation, decide approximately when and where two bodies may collide, and provide this information to the simulation program. The collision process is also very accurate if the surface properties k and δ are known, and coefficients of restitution other than unity can be treated by special consideration of the normal component of the relative velocity.

Unfortunately, the depth of penetration δ and the collision duration are small, so that very small integration time steps are needed. This can also lead to undesirable computational requirements when large numbers of bodies are involved.

The objective of the present work is to develop a collision model applicable to the submunition dispersion problem, but without the computational requirements of the more detailed collision process model described above. The procedure will be to simulate the process that a human observer would use to detect bodies in contact and determine the contact point. This procedure will involve a decision hierarchy with successively more complex calculations leading to the prediction of the collision point. The decision hierarchy serves the same purpose, computationally, as the "man-in-the-loop" mode described above.

Once the contact point has been determined, general vector equations are derived which exactly determine the linear and angular momentum exchange between bodies during an arbitrary 3-D collision. These equations include coefficients of restitution other than unity. To the author's knowledge, this is the first time that these equations have appeared in literature. Since the duration of impact is considered infinitesimal, collision effects may be determined exactly during one integration time step of a trajectory simulation.

The body description model used for determining contact points in the present work is restricted to bodies of revolution, which are modeled as axial distributions of spheres. However, the decision hierarchy and the momentum exchange equations can both be used with more complex body description models such as that of Refs. 14 and 15.

Simulation of Human Observation to Determine Collision Points

Given the location and orientation of two general bodies at an instant in time, what process would an outside observer use to determine if they were in contact? The first step is what could be called the relative distance test. The observer decides whether or not the relative distance between the bodies is greater than a representative body dimension, and if so, eliminates the pair from further consideration. A computer simulation can accomplish this process by finding the minimum diameter sphere which can enclose each body, and comparing the relative distance between bodies against the sum of the sphere radii.

The second step is the body orientation test. Assuming that the spheres enclosing each body overlap, the observer then decides whether or not the bodies are oriented such that they may be in contact. This process is simulated by enclosing each body in a finite length, minimum volume cylinder. The axis of the cylinder corresponds to the longitudinal axis of symmetry of the body, and the cylinder diameter is just sufficient to enclose all points of the body. If both cylinders share a common volume, then it is possible that the actual bodies are in contact.

If the body orientation test is positive, the observer views the bodies from various aspects and in effect performs a visual iteration process which terminates at the contact point. Simulation of this process requires a computer routine in which each body is represented by a number of discrete elements, such as spherical segments or plates. The routine must consider each pair of elements on the two bodies, determine which pair or pairs are in contact, and at what point. The above considerations define the simulation collision test procedure. The appropriate equations for each step will be discussed in subsequent sections.

Relative Distance Test

The motion of a single point on one body relative to a small planar surface on another body is a complex path in space and time. Due to the combination of translation and rotation, prediction of the actual time at contact in a simulation involves the solution of a transcendental equation. This is not computationally feasible for large numbers of bodies even if the body shape is relatively simple. With due consideration for computational economy, it was decided to merely test bodies for contact or overlap at the end of each integration time step. This restricts the procedure to a static interference model; however, if the time steps are sufficiently small, the overlap during collision will be insignificant and the true dynamic behavior adequately simulated.

In the static check case, the relative distance test is extremely simple. Consider two bodies, A and B, enclosed by spheres of radii r^A and r^B, respectively. If the inertial coordinates of the center of each sphere are given by R_i^A and R_i^B, their separation is

$$R_i = R_i^A - R_i^B \tag{1}$$

A collision is indicated when

$$R_i R_i \leq (r^A + r^B)^2 \tag{2}$$

Body Orientation Test

If the relative distance test is positive, the next step is the body orientation test. The classical method to determine whether two finite cylinders are in contact is to construct a vector from the surface of one cylinder to the surface of the other. If the cylinders are in contact, the length of this vector must be zero at one or more points on each surface. Unfortunately, the equations used in this process are lengthy and complex, and for certain orientations, singular.

A much simpler and computationally more efficient method can be obtained by simulating a visual process. With reference to Fig. 1, consider again two bodies A and B, now enclosed by cylinders of lengths L^A, L^B and radii r^A, r^B, respectively. The inertial coordinates of the centroids of each cylinder are R_i^A and R_i^B, and the separation of the centroids is given by Eq. (1). If the direction cosines of each body are

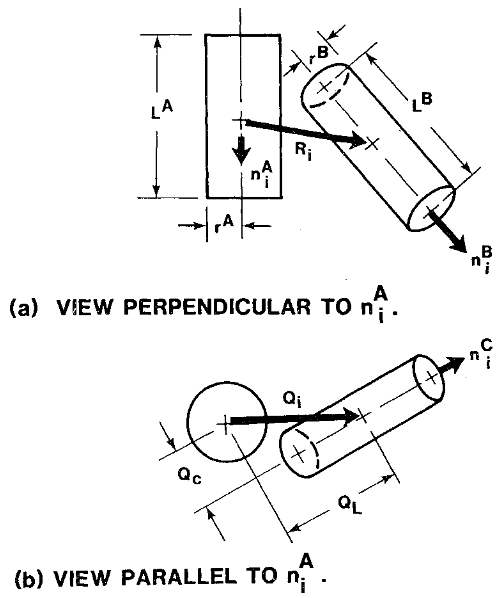

(a) VIEW PERPENDICULAR TO n_i^A.

(b) VIEW PARALLEL TO n_i^A.

Fig. 1 Body orientation test geometry.

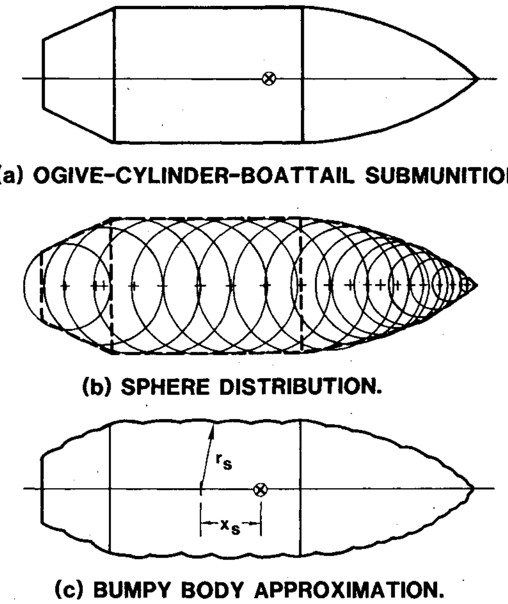

(a) OGIVE-CYLINDER-BOATTAIL SUBMUNITION.

(b) SPHERE DISTRIBUTION.

(c) BUMPY BODY APPROXIMATION.

Fig. 2 Body of revolution approximation.

known, the axial unit vectors for each cylinder are

$$n_i^A = b_{1i}^A \tag{3}$$

with an identical expression for body B.

From the geometry of Fig. 1,

$$Q_i = R_i - (R_k n_k^A) n_i^A \tag{4}$$

and

$$n_i^C = n_i^B - (n_k^B n_k^A) n_i^A \tag{5}$$

Although end effects are not exact, cylinder B shares a common volume with the infinite cylinder containing A if

$$Q_c^2 \le (r^A + r^B)^2 \tag{6a}$$

and

$$Q_L^2 \le [\tfrac{1}{2} L^B L(n_i^c) + r^A + r^B \sqrt{1 - n_i^c n_i^c}\,]^2 \tag{6b}$$

where

$$Q_L = Q_i n_i^c / L(n_i^c) \tag{7a}$$

$$Q_c^2 = Q_i Q_i - Q_L^2 \tag{7b}$$

and $L(n_i^c)$ is the scalar length of n_i^c.

If both Eqs. (6a) and (6b) are satisfied, the same sequence of computations are performed with n_i^A and n_i^B switched. If Eqs. (6a) and (6b) are satisfied for this case, then the two cylinders must share a common volume, and the body orientation test is positive. The next step is to determine the actual collision point on the body.

Body of Revolution Model

Determination of the actual collision point requires some model of the body surface with which the computer can work. An obvious approach would be to represent the body with planar polyhedral patches. The representation of the body could be made as accurate as desired by using a large number of small patches. Unfortunately, this approach would require large amounts of storage, and testing each pair of patches on two bodies for collision would require enormous computation times. Since collision between spheres is simple to predict, it would be desirable to use some sort of body representation based on spheres. Figure 2 illustrates how a typical body of revolution can be approximated by distributing spheres of varying radii along the longitudinal axis. For two bodies, determination of the collision point consists of testing each pair of spheres in the two bodies using equations similar to Eqs. (1) and (2). The separation between a sphere in body A and one in body B is given by

$$R_i = R_i^A + x_s^A b_{1i}^A - R_i^B - x_s^B b_{1i}^B \tag{8}$$

where R_i^A, R_i^B are the inertial coordinates of the center of gravity (c.g.), x_s^A, x_s^B are the longitudinal locations of the sphere centroids relative to the body c.g.'s, and b_{1i}^A, b_{1i}^B are the direction cosines of the body axes-of-symmetry. Two spheres are in contact if

$$R_i R_i \le (r_s^A + r_s^B)^2 \tag{9}$$

The collision point coordinates are given approximately by

$$r_i = R_i^B + x_s^B b_{1i}^B + \left(\frac{r_s^B}{r_s^A + r_s^B}\right) R_i \tag{10}$$

and the unit outward normal on body B at the collision point is

$$n_i = R_i / \sqrt{R_k R_k} \tag{11}$$

When more than one pair of spheres are in contact, the collision point may be approximated by averaging the values computed from Eq. (10)

Elastic Collisions of Two Bodies

Once the collision point is known, the only remaining problem is to determine the exchange of linear and angular momentum between the colliding bodies. Consider again two bodies, A and B, whose positions, velocities, and angular rates at the instant of collision are all known. Assume that the collision point and the unit outward surface normal vector at the collision point is known on at least one body. Further, assume that the collision is perfectly elastic, that the body surfaces are frictionless so that no shear forces act during the collision process, and that the duration of the contact is vanishingly small. It is then possible, using conservation of energy and momentum equations for the two-body system, to determine uniquely the velocities and angular rates of both bodies after the collision in terms of the known values prior to the collision.

Referring to the notation in Fig. 3, conservation of linear momentum before and after the collision gives

$$P_i^A + P_i^B = C_i \qquad \text{constant} \tag{12}$$

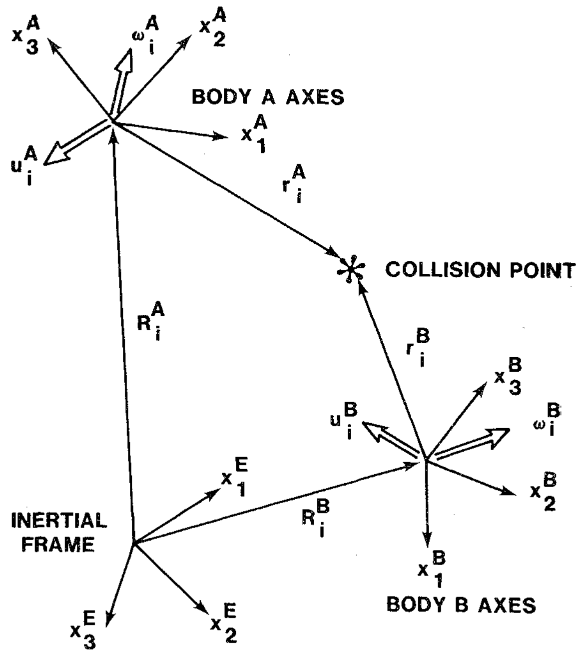

Fig. 3 Collision geometry.

where the momentum P_i of each body in the inertial frame is

$$P_i = mu_i \tag{13}$$

Defining the impulse due to the force acting during the collision interval as

$$G_i = \int_t^{t+\Delta t} f_i \mathrm{d}t \qquad \Delta t \ll 1 \tag{14}$$

then, in the inertial frame, the impulse on body A is

$$G_i^A = -G^A n_i^A \tag{15}$$

where n_i^A is the unit outward normal and G^A is the scalar magnitude of G_i^A. The momentum of body A after the collision is related to the momentum before the collision by

$$P_i^A(t+\Delta t) = P_i^A(t) - G^A n_i^A \tag{16}$$

Conserving momentum for the two-body system results in

$$G^A = G^B = G \tag{17}$$

and

$$n_i^A + n_i^B = 0 \tag{18}$$

Equations (17) and (18) state that the magnitude of the impulse acting on each body is the same, while the directions are equal and opposite. Also, the unit surface normal only needs to be found for one body, and Eq. (18) can be used to define it for the other.

The angular momentum of the two-body system, as computed about the system center of mass, is constant. Although the proof is tedious, it is obvious that the system angular momentum must remain constant since the net moment on the system is zero.

Conservation of kinetic energy for the system provides the final necessary relation for finding the scalar magnitude G of the impulse. The energy equation is a scalar equation and is frame independent. Since the angular rates and moments of inertia for each body are usually known in body-axis coordinates, body axes will be used to compute the rotational energy terms. The kinetic energy of translation for body A is

$$E_T^A = P_i^A P_i^A / 2m^A \tag{19}$$

Before the collision,

$$E_T^A(t) = P_i^A(t) P_i^A(t) / 2m^A \tag{20}$$

and after the collision, using Eq. (16)

$$E_T^A(t+\Delta t) = E_T^A(t) - G n_i^A [2P_i^A(t) - G n_i^A] / 2m^A \tag{21}$$

with an identical expression for body B. Similarly, the kinetic energy due to rotation is

$$E_R^A = \tfrac{1}{2} H_i^A \omega_i^A = \tfrac{1}{2} I_{ij}^A \omega_i^A \omega_j^A \tag{22}$$

The change in angular momentum of each body, measured in body axes with origin at the body c.g., is due to the moment caused by the collision impulse. This impulsive moment is

$$\int_t^{t+\Delta t} r_j f_k \epsilon_{ijk} \mathrm{d}t = -r_j G_k \epsilon_{ijk} \tag{23}$$

Defining the moment arm vector in body axes as

$$q_i = r_j n_k \epsilon_{mjk} b_{im} \tag{24}$$

the angular momentum after the collision is

$$H_i^A(t+\Delta t) = H_i(t) - G q_i^A \tag{25}$$

Introducing the inverse of the inertia tensor, J_{ij}, defined such that

$$J_{im} I_{mk} = \delta_{ik} \tag{26}$$

the angular rates are then

$$\omega_i = J_{ij} H_j \tag{27}$$

and the rotational energy after the collision may be shown to be

$$E_R^A(t+\Delta t) = E_R^A(t) - G q_i^A \omega_i^A + \tfrac{1}{2} G^2 J_{ij}^A q_i^A q_j^A \tag{28}$$

Equating total system energy before and after the collision

$$\begin{aligned} &E_T^A(t+\Delta t) + E_R^A(t+\Delta t) + E_T^B(t+\Delta t) + E_R^B(t+\Delta t) \\ &= E_T^A(t) + E_R^A(t) + E_T^B(t) + E_R^B(t) \end{aligned} \tag{29}$$

and solving for G results in

$$G = 2[n_i^A u_i^A + n_i^B u_i^B + q_i^A \omega_i^A + q_i^B \omega_i^B] \Big/ \left[\frac{1}{m^A} + \frac{1}{m^B} + q_i^A J_{ij}^A q_j^A + q_i^B J_{ij}^B q_j^B\right] \tag{30}$$

Coefficient of Restitution

For collisions in which the coefficient of restitution is less than unity, an equation for G similar to Eq. (30) may be derived. Using the defining equation for the coefficient of restitution C_R:

$$V_{\mathrm{REL}}(t+\Delta t) = -C_R V_{\mathrm{REL}}(t) \tag{31}$$

where the relative velocity at the collision point is

$$V_{\mathrm{REL}} = (v_i^A - v_i^B) n_i \tag{32}$$

and v_i, the inertial velocity of the collision point, is given by

$$v_i = u_i + \omega_m b_{mj} r_k \epsilon_{ijk} \tag{33}$$

Either n_i^A or n_i^B may be used in Eq. (32). From Eq. (16)

$$u_i^A(t+\Delta t) = u_i^A(t) - G n_i^A / m^A \tag{34}$$

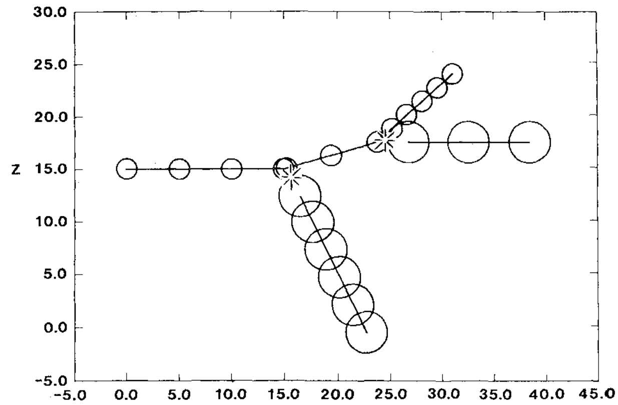

Fig. 4 Elastic sphere collisions.

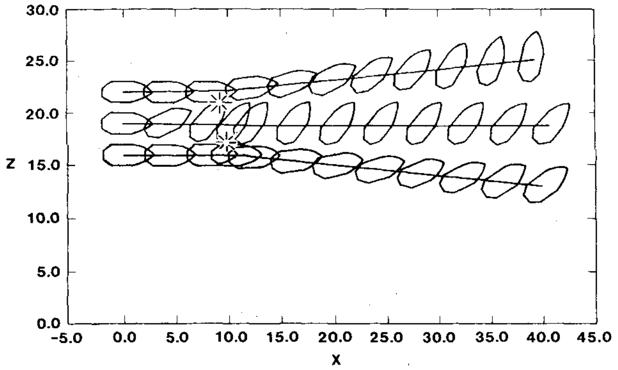

Fig. 5 Submunition collisions.

and from Eq. (25)

$$\omega_i^A(t+\Delta t) = \omega_i^A(t) - GJ_{ij}^A q_j^A \tag{35}$$

with similar expressions for body B. Substituting the above forms into Eq. (31) and solving G gives

$$G = [1+C_R]\,[n_i^A u_i^A + n_i^B u_i^B + q_i^A \omega_i^A + q_i^B \omega_i^B]$$

$$\div \left[\frac{1}{m^A} + \frac{1}{m^B} + q_i^A J_{ij}^A q_j^A + q_i^B J_i^B q_j^B\right] \tag{36}$$

Note that Eq. (36) reduces to Eq. (30) when C_R is unity. Equation (36) cannot be used, however, unless C_R between the colliding materials at the collision point is known. Once G is determined from either Eq. (30) or Eq. (36), the postcollision velocities and angular rates are given by Eqs. (34) and (35).

Results and Conclusions

When the collision impulse moment arm q_i is zero, Eqs. (30) and (36) are valid only for spherical bodies, and some closed-form solutions can be obtained. For example, when $m^A = m^B$, $C_R = 0$, $u_i^A = (V,0,0)$, and $u_i^B = (0,0,0)$, the postcollision velocities are $u_i^A = u_i^B = [V/2(0,0)]$. Also, for two arbitrary masses and $C_R = 1$, the well-known classical velocity exchange for spherical body collisions is obtained.

To validate both collision point prediction and momentum exchange for more complicated cases, the collision model and reaction equations were incorporated into a multiple-body six-degree-of-freedom trajectory simulation. Several numerical tests were performed; two simple illustrative examples are shown in Figs. 4 and 5.

Figure 4 illustrates the elastic collision of spherical bodies where a massive, small diameter sphere collides with two larger spheres of small mass. Specular collisions result, with the proper rebound angles and velocity exchanges accurately predicted.

A more general example is shown in Fig. 5, where three bodies of revolution with shapes similar to that of Fig. 2 are flying force-free trajectories. At time zero, all three bodies are translating horizontally, stacked one above the other, and the centerbody is given a positive pitch rate. The centerbody first collides with the upper body and then rebounds into the lower one. The dispersion effects of the collisions are readily apparent at the end of the trajectory.

The collision model has been used in more complex studies involving from 13 up to 72,200 bodies in motion simultaneously. The simulation program for these studies included not only the usual flight mechanics effects, such as gravity, aerodynamic coefficients, thrust and mass loss, but also launcher, rocket plume, and aerodynamic interference effects. In simulations of this magnitude, accuracy, speed, and efficiency are of paramount importance. Computation times on both a CDC 7600 and a VAX for several test cases such as these were increased only a few percent with the inclusion of the collision model.

In summary, an automated collision model has been developed for use in submunition dispersion simulations. The model consists of three distinct parts: a collision decision hierarchy, a solid body model, and exact momentum exchange equations. The collision decision hierarchy is a simulation of the human observation process for detecting bodies which may be in contact. The solid body model, which is presently restricted to bodies of revolution only, is used to determine actual contact or collision points. With the contact point known, the momentum exchange equations determine exactly the postcollision velocities and angular rates. The equations are valid for coefficients of restitution other than unity. From numerical tests, the entire procedure has been found to be fast, accurate, and computationally efficient.

Acknowledgment

This work was supported by the Department of Defense, Naval Surface Weapons Center, Dahlgren Laboratory, Dahlgren, Virginia.

References

[1] Brunk, J.E., "Flight Dynamics and Dispersion of Cluster Munitions," Technical Report 4835, Picatinny Arsenal, Dover, N.J., July 1975.

[2] Martin, F.W., Saunders, G.H., and Smith, C.J., "Image System Solution for Store Aerodynamics with Interference—Part I," *Journal of Aircraft,* Vol. 12, March 1975, pp. 151-155.

[3] Martin, F.W. and Walkley, K.B., "Image System Solution for Store Aerodynamics with Interference—Part II," *Journal of Aircraft,* Vol. 12, March 1975, pp. 156-161.

[4] Martin, F.W., Burkhalter, J.E., Purvis, J.W., and Martin, B.D., "Analysis and Comparison of Several Methods for Computing Aerodynamic Compressibility and Interference Effects up to Critical Mach Numbers," AFATL-TR-77-112, Eglin Air Force Base, Fla., Sept. 1977.

[5] Bayman, B.F., "Model of the Behavior of Solid Objects During Collision," *American Journal of Physics,* Vol. 44, No. 77, July 1976, pp. 671-676.

[6] Maryamor, A.N., "Calculation of a Collision Between Metallic Bodies from a Compressible-Liquid Model," *Zhurnal Prikladnoi Mekhaniki i Tekhnicheskoi Fiziki,* Vol. 8, No. 2, 1967, pp. 83-85.

[7] Lozano-Perez, T. and Wesley, M.A., "An Algorithm for Planning Collision-Free Paths Among Polyhedral Objects," *Communications of the ACM,* Vol. 22, Oct. 1979, pp. 560-570.

[8] Boyse, J.W., "Interference Detection Among Solids and Surfaces," *Communications of the ACM,* Vol. 22, Jan. 1979, pp. 3-9.

[9]Ishisaka, T., Tani, M., Fujii, O., and Hamada, K., "Analysis of Crashworthiness of Automobile Body in Collision (Simulation of Frontal Collision)," *Mitsubishi Heavy Industries Technical Review,* Vol. 132, No. 2, June 1976, pp. 125-131.

[10]Belli, V., "Considerations on the Duration of Impact, in Some Cases of the Integrability of the Equations of Motion, in a Collision Between Ships," *Tecnica Italiana Rivista di Ingegneria,* Vol. 44, No. 3, May-June 1979, pp. 163-166.

[11]Brach, R.M., "Impact Moment Coefficient for Vehicle Collision Analysis," SAE Paper 770014, Feb.-March 1977.

[12]Chubb, W.B., "The Collision Boundary Between the Two Separating Stages of the SA-4 Saturn Vehicle," NASA TN-D-598, Marshall Space Flight Center, Aug. 1961.

[13]Peotter, G. and Bloomgren, P., "Program 624A—Standard Space Launch Vehicle Staging Dynamics Analysis Report—Flight Test Plan VIII," Aerospace Division of Martin-Marietta Corporation, Denver, Colo., Feb. 1965.

[14]Richter, B.J., "A Description of the Computer Program DYNAMITE," LMSC-D436926, Lockheed Missiles and Space Company, Inc., Palo Alto, Calif., Dec. 1975.

[15]Culp, M.F., Morris, G.W., and Welch, B.H., "Dynamic Interaction Simulation of Clustered Ordnance Aerodynamic Loading Base," AFATL-TR-79-88, Air Force Armament Laboratory, Eglin AFB, Fla., Oct. 1979.